J. Biochem. **144,** 487–497 (2008)
doi:10.1093/jb/mvn092

A Plasma Membrane-associated Protein of *Arabidopsis thaliana* AtPCaP1 Binds Copper Ions and Changes Its Higher Order Structure

Nahoko Nagasaki-Takeuchi[1,*], Masashi Miyano[2] and Masayoshi Maeshima[1,†]

[1]Laboratory of Cell Dynamics, Graduate School of Bioagricultural Sciences, Nagoya University, Nagoya, 464-8601; and [2]Structural Biophysics Laboratory, RIKEN SPring-8 Center, Harima Institute, Kouto, Sayo, Hyogo, 679-5148, Japan

Received June 4, 2008; accepted July 9, 2008; published online July 29, 2008

PCaP1, a hydrophilic cation-binding protein, is bound to the plasma membrane in *Arabidopsis thaliana*. We focused on the physicochemical properties of PCaP1 to understand its uniqueness in terms of structure and binding of metal ions. On fluorescence analysis, PCaP1 showed a signal of structural change in the presence of Cu^{2+}. The near-UV CD spectra showed a marked change of PCaP1 in $CuCl_2$ solution. The far-UV CD spectra showed the presence of α-helices and the intrinsically unstructured region. However, addition of Cu^{2+} gave no change in the far-UV CD spectra. These results indicate that Cu^{2+} induced a change in the tertiary structure without changing the secondary structure. The protein was sensitive to proteinase in the presence of Cu^{2+}, supporting that Cu^{2+} is involved in the structural change. The PCaP1 solution was titrated with $CuCl_2$ and the change in the fluorescence spectrum was monitored to characterize Cu^{2+}-binding properties. The obtained values of K_d for Cu^{2+} and the ligand-binding number were 10 μM and six ions per molecule, respectively. These findings indicate that PCaP1 has a high Cu^{2+}-binding capacity with a relatively high affinity. PCaP1 lacks cysteine and histidine residues. A large number of glutamate residues may be involved in the Cu^{2+} binding.

Key words: cation-binding protein, circular dichroism, copper, fluorescence, plant.

Abbreviations: CD, circular dichroism; DSC, differential scanning calorimetry; PCaP1, plasma membrane-associated cation-binding protein; $PI(3,5)P_2$, phosphatidylinositol 3,5-bisphosphate; $PI(3,4,5)P_3$, phosphatidylinositol 3,4,5-triphosphate.

Copper is an essential micronutrient in plants, and plays an important role in photosynthetic and respiratory electron-transport chains in chloroplasts and mitochondria, respectively. Copper is also involved in crucial biological processes including ethylene perception, cell-wall metabolism and protection from oxidative stresses. The intracellular level of copper ion is precisely regulated to prevent damage caused by reactivity with sulphhydryl groups and formation of free radical species (*1*). In cells, copper ion can exist in two chemical states, Cu^{2+} and Cu^{+}. Copper ions in cells are bound to copper-binding proteins and enzymes. Superoxide dismutase, cytochrome *c* oxidase and ascorbate peroxidase have been known as metalloenzymes with copper. Ethylene receptor (*2*), Sco (*3*) and S100b (*4*) have been identified as copper-binding proteins. Especially, several regulatory copper-containing proteins have high affinity for copper ion and function to avoid toxic side reactions of copper ion in the cell (*5*). Previously, we reported a new type of cation-binding protein associated with the plasma membrane of *Arabidopsis thaliana* (AtPCaP1, hereafter referred to as PCaP1) (*6*). Here, we report its high copper-binding capacity.

Copper is required in various locations in the plant cell: namely, the cytosol, mitochondrial inner membrane and chloroplast (*7*). Plant cells have copper-transport systems including copper chaperon and copper-binding protein to deliver copper ion to these proper organelles. Protein components involved in the copper homeostasis have been found in *A. thaliana*. Several proteins function as membrane transporters for copper ion, such as copper transporter protein (COPT)-family transporter (*8*, *9*) and heavy metal P-type ATPase (HMA) (*10*, *11*). The ion selectivity of these membrane transporters varies with the molecular species. Once inside the cell, Cu^{+} and Cu^{2+} are transported to the proper organelles or components by the soluble copper receptors that are named copper chaperones (*5*). Three copper chaperones have been found in plants and are well characterized; namely, ATX1, CCS and COX17 (*12*–*15*). ATX1 delivers copper to the secretory pathway via a copper-transporting P-type ATPase (*16*, *17*), and CCS delivers copper to Cu/Zn superoxide dismutase (*18*, *19*). COX17 deliver copper to mitochondria for cytochrome *c* oxidase (*20*). Recently, a chloroplast copper-binding protein CUTA was found in *A. thaliana* (*14*). These proteins are different from the cysteine-rich metal-binding peptides, such as metallothionein and

*Present address: Graduate School of Biological Sciences, Nara Institute of Science and Technology, Takayama, Ikoma, Nara 630-0129, Japan.
†To whom correspondence should be addressed. Tel/Fax: +81-52-789-4096, E-mail: maeshima@agr.nagoya-u.ac.jp

phytochelatin, in their molecular size and physiological role (*21*).

The primary structure of PCaP1 is different from these metal chaperones and copper-binding proteins. Furthermore, PCaP1 has no cysteine and histidine residues, which are essential for copper-binding function in most copper-binding proteins. This protein has been reported to be stably associated with the plasma membrane via *N*-myristoylation and to interact with calmodulin/Ca^{2+} complex and phosphatidylinositol phosphates, especially $PI(3,4,5)P_3$ and $PI(3,5)P_2$ (*22*). The PCaP1 gene was constitutively expressed in all major tissues and the mRNA level increased after the treatment with a pathological elicitor, copper and sorbitol at a high concentration (*6*). The physiological role of PCaP1 is presently unknown. Here, we prepared a highly purified recombinant PCaP1 and investigated the biochemical and physicochemical properties, especially metal-binding properties. Here, we discuss the biochemical evidence for binding of Cu^{2+} to PCaP1 and its biochemical and physiological meanings for copper homeostasis and detoxification in plant cells.

MATERIALS AND METHODS

Preparation of Recombinant PCaP1—Constructs for PCaP1 tagged with His (PCaP1/His) (*6*) and PCaP1 (*22*) were prepared and introduced into *Escherichia coli* BL21(DE3) using the pET23b expression vector (Novagen, WI, USA) as described previously. The obtained expression vector pET/PCaP1/His was introduced into *E. coli* BL21(DE3). Transformants were grown in LB broth for 2 h at 25°C after induction with 1 mM isopropyl-thio-β-D-galactoside.

Purification of Recombinant Proteins—PCaP1 was purified as described previously (*22*). *Escherichia coli* cells expressing PCaP1/His were harvested and then disrupted by sonication for 12.5 min on ice. After removal of cell debris by centrifugation at 104,000*g* for 30 min, the supernatant was applied to a Ni-NTA Superflow column (Qiagen, Valencia, CA, USA). Recombinant PCaP1/His was eluted with 300 mM imidazole containing 20 mM Tris–acetate (pH 7.5) and 2 M NaCl. The content of PCaP1 was measured by immunoblotting with an anti-PCaP1 antibody. The PCaP1-enriched fractions were collected and applied to a HiTrap Phenyl HP column (GE Healthcare, NJ, USA). PCaP1/His was recovered in the flow-through fraction and desalted. To prepare PCaP1, we removed the $(His)_6$ tag from PCaP1/His by treatment with TAGZyme (Qiagen). Then, PCaP1 was applied to a column (2.6 × 60 cm) of Sephacryl S-300 HR (GE Healthcare). The purified preparation of PCaP1 was used for all experiments in the present study. Protein concentration was determined using BCA Protein Assay Reagent Kit (Pierce Biotechnology, CA, USA). The purity of the preparation was examined by sodium dodecyl sulphate (SDS)–PAGE in a 12.5% (w/v) polyacrylamide gel.

$^{45}Ca^{2+}$ Overlay Assay—The effect of heat treatment on Ca^{2+} binding of PCaP1 was determined by $^{45}Ca^{2+}$ overlay assay (*23*, *24*). PCaP1 was spotted onto a polyvinylidene fluoride (PVDF) membrane. The membrane was rinsed, incubated in the buffer supplemented with 1 mM $CaCl_2$ and 3.7 MBq of $^{45}Ca^{2+}$ (as $CaCl_2$) at 23°C for 30 min, washed twice with 10 ml of 50% (v/v) ethanol, and then dried. An autoradiogram of the $^{45}Ca^{2+}$-labelled proteins on the membrane was obtained by exposure to an X-ray film for 3 days at –80°C.

Analytical Gel Filtration Column Chromatography—PCaP1 (16 μM, 0.5 ml) was applied to a column (1.0 × 30 cm) of Superdex-200 (GE Healthcare) set in an ÄKTA FPLC (GE Healthcare). The column was equilibrated with 10 mM Tris–HCl (pH 7.5), and 150 mM NaCl with or without 1 mM $CaCl_2$, $MgCl_2$ or $CuCl_2$.

Proteolytic Digestion Assay—PCaP1 was treated with V8 proteinase, a *Staphylococcus aureus* serine proteinase (Wako Fine Chemicals, Osaka, Japan) at 37°C in the presence of 3.3 mM $CuCl_2$, $CaCl_2$ or $MgCl_2$. The molar ratio of PCaP1 to V8 protease was 5000 : 1. The reaction was stopped by the addition of 2% SDS, 6% glycerol, 2% mercaptoethanol and 10 mM Tris–HCl (pH 6.8). The proteolytic digestion was measured by SDS–PAGE. The staining intensity of 36 kDa band of PCaP1 was measured using an ATTO Light Capture AE-6961 densitometer (Tokyo, Japan).

Fluorescence Spectroscopy—Fluorescence spectroscopy was performed using a Shimadzu RF-5300PC fluorescence spectrophotometer (Kyoto, Japan) set at 277 nm for excitation. The slit widths for emission and excitation were set at 5 and 10 nm, respectively. The protein concentration of PCaP1 was 0.81 μM in 10 mM Tris–HCl (pH 7.5). Emission spectra were acquired from 280 to 470 nm. To examine the reversibility of binding of PCaP1 to Cu^{2+}, we mixed PCaP1 with 2 mM $CuCl_2$ and then removed Cu^{2+} by adding 28 mM Na–EDTA. The sample solution was dialysed against 10 mM Tris–HCl (pH 7.5) and then washed three times using a Vivaspin ultrafiltration spin column (Vivascience, Hanover, Germany). The obtained PCaP1 sample was subjected to fluorescence analysis with Cu^{2+}. The effect of other ions was examined by titrating $CuCl_2$ against PCaP1 in the presence of 1 mM KCl, $CaCl_2$ or $MgCl_2$.

The dissociation constant (K_d) and the stoichiometry (n) were determined using the fluorescence titration curve of the binding of Cu^{2+} to PCaP1. The copper concentration-dependent fluorescence intensity change of the PCaP1 was interpreted by the following equations as described for Ca^{2+}-binding protein (*25–27*).

The Cu^{2+} binding of PCaP1,

$$PCaP1 + Cu^{2+} \leftrightarrows PCaP1{:}Cu^{2+}$$

is written as the equation,

$$K_d = \frac{[PCaP1][Cu^{2+}]}{[PCaP1{:}Cu^{2+}]} \quad (1)$$

where, K_d is the dissociation constant of $[PCaP{:}Cu^{2+}]$. Since the fluorescence intensity change ($F_0 - F$) is proportional to $[PCaP1{:}Cu^{2+}]$, Eq. 1 can be written as follows,

$$(F_0 - F) = \frac{(\Delta F_{max} \times [Cu^{2+}])}{(K_d + [Cu^{2+}])} \quad (2)$$

where, F_0 and F, fluorescence intensity at 344.8 nm in the absence or presence of Cu^{2+}, respectively; ΔF_{max}, the

maximum fluorescence change observed when the protein is fully occupied at the specific Cu^{2+}-binding sites with an affinity of K_d in a binding site-independent manner; [Cu^{2+}] and [PCaP1], concentrations of free Cu^{2+} and PCaP1 in the reaction mixture, respectively. The validity of Eq. 2 was confirmed by the linearity of the plot of $1/(F_0 - F)$ versus $1/[Cu^{2+}]$ in the following equation (Fig. 8).

$$\frac{1}{F_0 - F} = \frac{K_d}{\Delta F_{max} \times [Cu^{2+}]} + \frac{1}{\Delta F_{max}} \quad (3)$$

In this analysis, we applied the following equation to calculate the ligand-binding number (n) with assumption that the PCaP1 has n identical binding sites with the same affinity.

$$\frac{1}{F_0 - F} = \frac{2n}{\Delta F_{max}} \times \frac{1}{[Cu^{2+}]/[PCaP1]} + \frac{1}{\Delta F_{max}} \quad (4)$$

Absorption Spectroscopy—Absorption spectra of PCaP1 were taken with a Beckman DU 640 spectrophotometer (Beckman Coulter, CA, USA) using a 2 mm path-length quartz cuvette. All measurements were taken after incubation of PCaP1 (58.2 μM) with appropriate concentrations of $CuCl_2$ in 10 mM Tris–HCl (pH 7.5) for 2 min at 25°C. The background signal for the buffer supplemented with $CuCl_2$ was subtracted from that of the sample spectra. The data were analysed using KaleidaGraph ver.3.6 (Synergy Software, PA, USA).

Shift of absorbance wavelength of $CuCl_2$ solution in the presence of PCaP1 was measured. Values of wavelength shift are plotted according to the following equation.

$$\Delta\lambda = (\lambda_{without\text{-}50} - \lambda_{PCaP1\text{-}50}) - (\lambda_{without} - \lambda_{PCaP1})$$

where, $\Delta\lambda$, difference in the wavelength (nm); $\lambda_{without}$, peak wavelength of $CuCl_2$ solution without PCaP1 at the indicated concentration of $CuCl_2$; λ_{PCaP1}, peak wavelength in the presence of PCaP1 at the indicated concentration of $CuCl_2$, $\lambda_{without\text{-}50}$, peak wavelength in the absence of PCaP1 in 50 μM $CuCl_2$ (634 nm); $\lambda_{PCaP1\text{-}50}$, peak wavelength in the presence of PCaP1 in 50 μM $CuCl_2$ (565 nm).

Differential Scanning Calorimetry—Differential scanning calorimetry (DSC) was performed using a capillary differential scanning calorimeter VP-Capillary DSC (MicroCal, Northampton, MA, USA) as described previously (*25*). The scans were performed by increasing the temperature from 20°C to 70°C at a scan rate of 200°C h^{-1}. PCaP1 was dissolved in 10 mM Tris–HCl (pH 7.5) supplemented with 5 mM KCl, $SrCl_2$, $CaCl_2$ or $MgCl_2$. The final concentration of PCaP1 was 20.4 or 40.7 μM. The background signal for the buffer was subtracted from that of the sample spectra. The data were analysed using DSC data analysis modules in ORIGIN software version 7.0 (MicroCal, MA, USA).

Circular Dichroism Spectroscopy—The ellipticity was followed with a J-725 spectropolarimeter (Jasco, Tokyo, Japan) equipped with a PTC-348WI temperature controller (Jasco) (*25*). The concentrations of protein samples applied were 7.3 μM for far-UV CD spectra and 40.7 μM for near-UV CD spectra in 10 mM Tris–HCl (pH 7.5). Far-UV CD spectra of samples (0.5 ml) were measured in a range of 190–250 nm with a light path length of 1 mm in the presence or absence of 0.6 mM $CuCl_2$. All spectra are shown as the average of five scans. Near-UV CD spectra of samples (1.5 ml) were measured at a range of 320–240 nm with a light path length of 10 mm in the presence or absence of 0.13 mM $CuCl_2$. All spectra are shown as the average of 10 scans. In both cases, the background signal for the buffer was subtracted from that of the sample spectra. The data were analysed using KaleidaGraph ver.3.6 (Synergy Software).

RESULTS

Effect of Metal Ions on Stability of PCaP1 Structure—PCaP1 was found as a calcium-binding protein (*6*). To study the effect of metal ions on the PCaP1 structure, we prepared a large quantity of recombinant PCaP1 without any tag sequence in a highly purified form. Quality of the PCaP1 preparation has been confirmed as described previously (*22*). DSC spectra show broad transition of excess heat capacity with transition temperature, T_m, shifts in concentration and metal-dependent manner but no change of total specific excess heat capacities (Fig. 1A). The excess heat capacity transitions in DSC

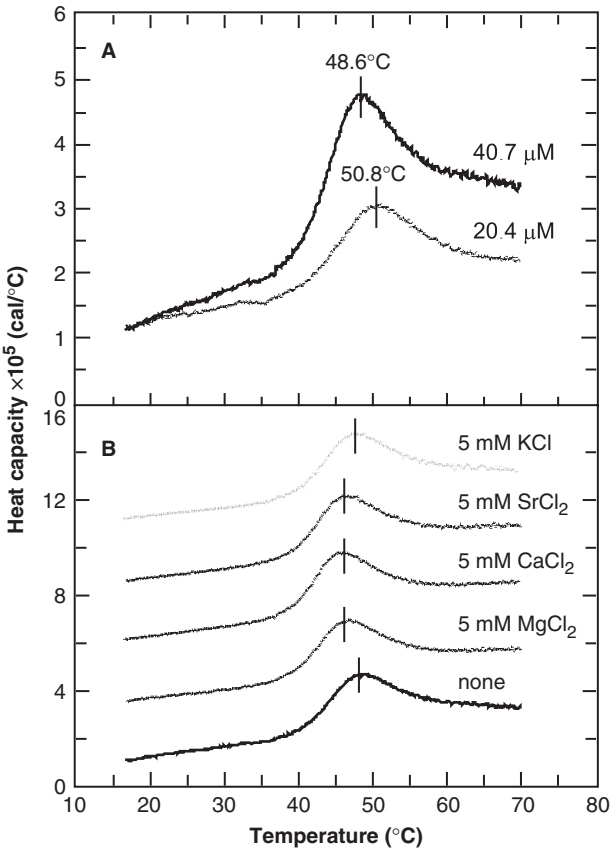

Fig. 1. **Differential scanning calorimetry of PCaP1.** (A) DSC thermograms of PCaP1 at protein concentrations of 20.4 and 40.7 μM. Vertical lines indicate peaks of heat capacity. (B) DSC thermograms of PCaP1 (concentration, 40.7 μM) were recorded in the presence of KCl, $SrCl_2$, $CaCl_2$ or $MgCl_2$ at 5 mM. The heating rate was 200°C h^{-1} in 10 mM Tris–HCl (pH 7.5). Curves mean the dependence of excess heat capacity, C_p. The curves of each scan are offset for clarity.

measurements indicate that PCaP1 is folded protein in a part at least, and PCaP1 is denatured by heat. The T_m value was slightly shifted from 48.6°C to 50.8°C when the PCaP1 concentration was diluted from 40.7 to 20.4 μM, whereas the all profiles of the excess heat capacity changes were superimposable in the heat denaturation of the solutions with the same protein concentration. The T_m of PCaP1 in DSC was shifted larger in the measured divalent cations including Sr^{2+}, Ca^{2+} or Mg^{2+} at around 46°C than the change in that of monovalent cation K^+ at 48.1°C from the absence of cation at 48.6°C (Fig. 1B, Table 1). K^+ had a much weaker effect than the other divalent metal ions. In all cases, the T_m at 20.4 μM PCaP1 was higher than that at 40.7 μM (Table 1).

It should be noted that PCaP1 showed the same DSC spectra as the original spectra when PCaP1 was re-examined after heat treatment (data not shown). As shown in Fig. 2, PCaP1 retained Ca^{2+}-binding capacity even after heating at 95°C for 10 min.

Change in Fluorescence Spectrum of PCaP1 Caused by Copper—Tryptophan and tyrosine residues are generally used as probes of the protein conformation because the microenvironment of these residues is reflected in fluorescence spectrum of the protein. PCaP1 has a single tryptophan residue at the fourth position of the sequence and four tyrosine residues (*6*). PCaP1 showed two peaks at 308.4 and 344.8 nm when excited at 277 nm (Fig. 3A). The peak at 308.4 nm might not be water Raman spectrum peak, because the spectrum of the buffer was subtracted from each spectrum of the PCaP1 solution. This peak may reflect the fluorescence emission of tyrosine residues. The peak fluorescence at 344.8 nm is typical for tryptophan residue exposed to the water solution (*26*). In general, the fluorescence is enhanced for the protein containing both tryptophan and tyrosine residues, because the fluorescence from tyrosine residue is absorbed by tryptophan residue.

The fluorescence emission spectrum of PCaP1 was markedly changed when Cu^{2+} was added into the protein solution at 19 μM. In contrast, K^+, Ca^{2+}, Mg^{2+}, Co^{2+} and Sr^{2+} gave no effect (Fig. 3A and B). Fluorescence at 344.8 nm of PCaP1 was decreased in a Cu^{2+} concentration-dependent manner (Fig. 3C). The fluorescence was gradually decreased and reached 12% of the original fluorescence when Cu^{2+} solution was added to the PCaP1 solution. In general, quenching of fluorescence occurs in the presence of metal ions. However, the effect by copper ion was remarkable. The decrease in the fluorescence in the presence of other metal ions was only 25%. This may be due to the dilution effect in this experiment, because this change was also observed even in the buffer without metal ions. These results strongly suggest the conformational change by Cu^{2+}, at least change in the conformation of the vicinity of tryptophan and tyrosine residue.

Change in Molecular Size and/or Shape—Change in apparent molecular size of PCaP1 by metal ions was examined by analytical gel filtration using a Superdex-200 column. PCaP1 showed a single peak of elution pattern and the peak was shifted to the larger portion by addition of 1 mM $CuCl_2$ (Fig. 4A). The apparent molecular sizes of PCaP1 with and without Cu^{2+} were roughly calculated to be 90 and 62 kDa as a spherical folded protein from the calibration curve (Fig. 4B). This result indicates that the apparent effective hydrodynamic radius increased in the presence of Cu^{2+}. The elution peak positions in the presence of Ca^{2+} and Mg^{2+} were the same as that with Cu^{2+}. Furthermore, the elution profile became sharp in the presence of these metal ions. These results suggest that the molecular size and/or shape of PCaP1 were slightly changed by the association with these metal ions.

Effect of Copper on the Secondary Structure of PCaP1—Changes in fluorescence spectra shown in Fig. 3 suggested the conformational change of PCaP1 caused by copper.

Thus, we determined the typical secondary structures and their changes by addition of Cu^{2+} by far-UV CD spectroscopy. Addition of 0.6 mM $CuCl_2$ did not affect the spectrum of PCaP1 significantly (Fig. 5A), suggesting that the secondary structure of PCaP1 was not changed by addition of Cu^{2+}. Then, we compared the spectra of near-UV CD spectrum of PCaP1 in the presence or absence of Cu^{2+}. The CD spectrum in the near-UV spectral region is sensitive to the tertiary structure of proteins and the CD signals at this wavelength region are attributable to aromatic amino acids: namely, phenylalanine, tyrosine and tryptophan. In contrast to the far-UV CD spectra, the binding of Cu^{2+} to PCaP1 changed the near-UV CD spectrum (Fig. 5B). These results indicate that binding of Cu^{2+} changed the tertiary

Table 1. **Effect of metal ions on transition temperature (T_m) of PCaP1.**

Salt	T_m of PCaP1 at	
	20.4 μM (°C)	40.7 μM (°C)
None	50.8	48.6
KCl	50.6	48.1
$SrCl_2$	49.4	46.5
$CaCl_2$	48.8	46.1
$MgCl_2$	49.2	46.7

The values of T_m are calculated from the DSC analysis in the presence of KCl, $SrCl_2$, $CaCl_2$ or $MgCl_2$ at 5 mM.

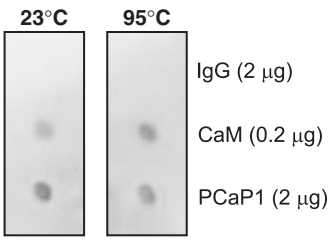

Fig. 2. **Effect of heat treatment on the Ca^{2+}-binding property of PCaP1.** PCaP1 (with or without heat treatment) was blotted onto a polyvinylidene fluoride membrane, and then the membrane was subjected to $^{45}Ca^{2+}$ overlay assay. Only PCaP1 was heated at 95°C for 10 min and then applied to a membrane (right panel). IgG (a negative control) and calmodulin (CaM, a positive control of calcium-binding protein) were not subjected to heat treatment in any cases as $^{45}Ca^{2+}$-binding reference.

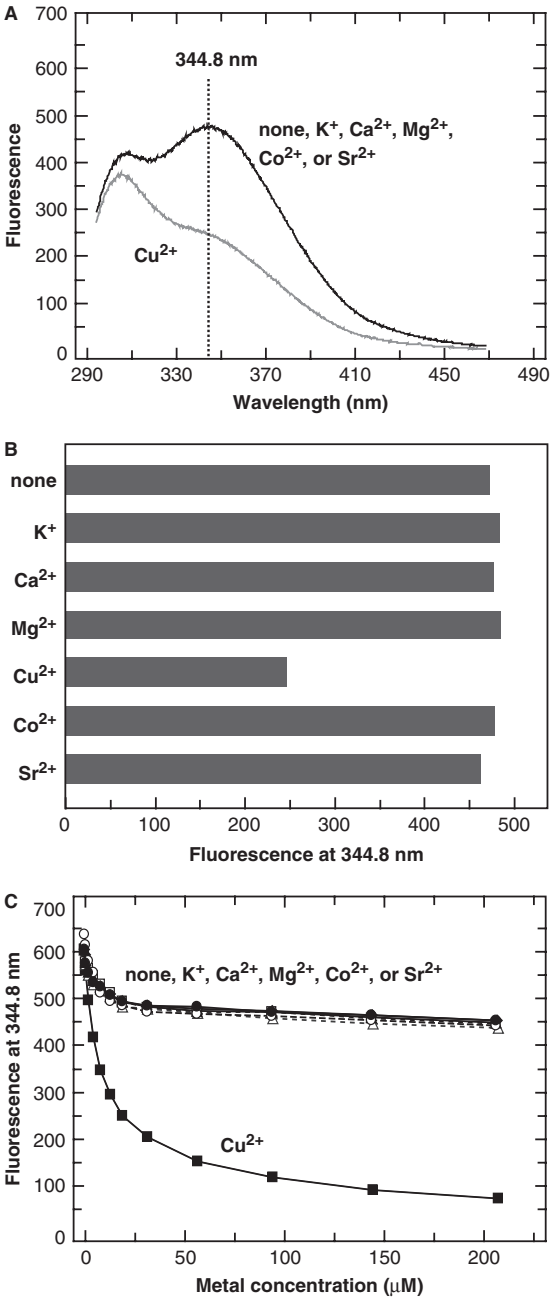

Fig. 3. **Fluorescence spectrum analysis of the effect of metal ions on the structure of PCaP1.** (A) Fluorescence emission spectra of PCaP1 obtained using a fluorescence spectrophotometer set at 277 nm for excitation. Spectra of PCaP1 (0.81 μM) in 10 mM Tris–HCl (pH 7.5) were monitored in the presence of 19 μM $CuCl_2$ or other ion, such as KCl, $CaCl_2$, $MgCl_2$, $CoCl_2$ or $SrCl_2$ (19 μM). The emission spectra in the presence of these ions were thoroughly consistent with the spectrum without metal ion (none). Fluorescence intensity is given in arbitrary unit. (B) Fluorescence of PCaP1 at 344.8 nm in the presence of metal ions. The fluorescence emission intensity at 344.8 nm of PCaP1 was measured after incubation with metal ion at 19 μM or without metal ion (none). (C) Concentration dependence of fluorescence emission of PCaP1 on the concentration of metal ions. Metal salts used were KCl (open circles), $CaCl_2$ (closed triangles), $MgCl_2$ (open triangles), $CuCl_2$ (closed squares), $CoCl_2$ (open triangles) and $SrCl_2$ (closed diamond). None (without metal salt), closed circles.

structure of PCaP1 in the vicinity of aromatic amino acid residues with no significant change in the secondary structure.

Heat Stability of Secondary Structure of PCaP1 in Cu^{2+}-binding Form—DSC experiment revealed that binding of metal ion decreased the heat stability (Fig. 1). DSC experiments require a high concentration of sample protein, under which Cu^{2+} causes aggregation of PCaP1. Thus, the change in far-UV CD spectrum of PCaP1 was measured at a relatively low concentration of protein sample in a temperature range of 20–70°C to

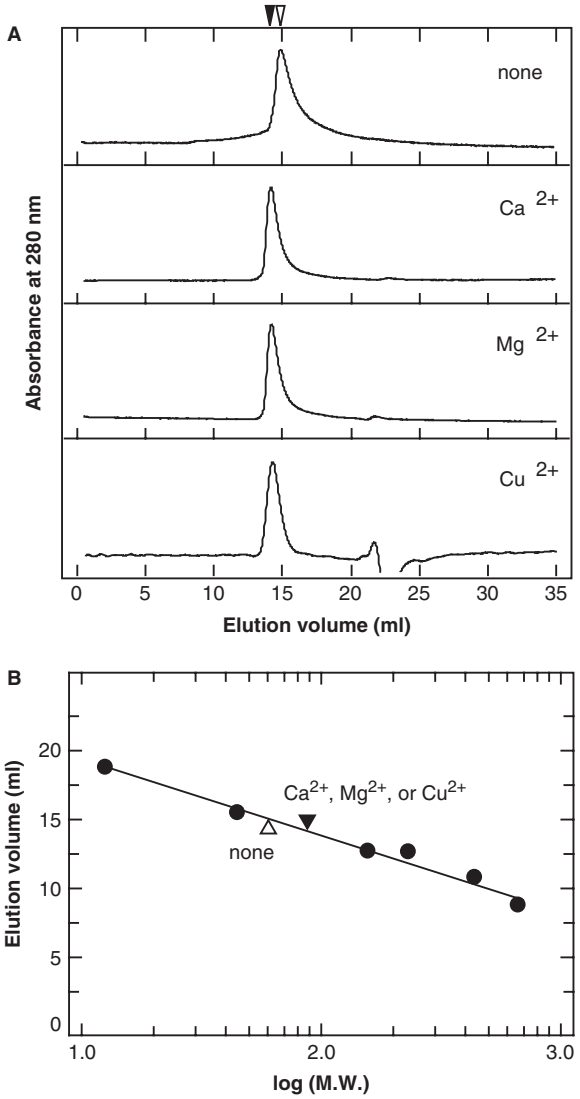

Fig. 4. **Analytical gel filtration of PCaP1.** (A) PCaP1 (16 μM, 0.5 ml) was applied to a Superdex200 column (1.0 × 30 cm) equilibrated in 10 mM Tris–HCl (pH 7.5) and 150 mM NaCl with $CaCl_2$, $MgCl_2$ or $CuCl_2$ at 1 mM. The same chromatography was done without metal ions as a control (none). Absorbance at 280 nm was monitored and shown as an arbitrary unit. The flow rate was maintained at 0.8 ml/min. (B) Calibration of apparent molecular size of PCaP1. The elution volumes of marker proteins and PCaP1 in the presence of metal ion were plotted against the molecular weight. Markers used were thyroglobulin (669 kDa), ferritin (440 kDa), catalase (232 kDa), aldolase (158 kDa), ovalbumin (45 kDa) and cytochrome c (12.5 kDa).

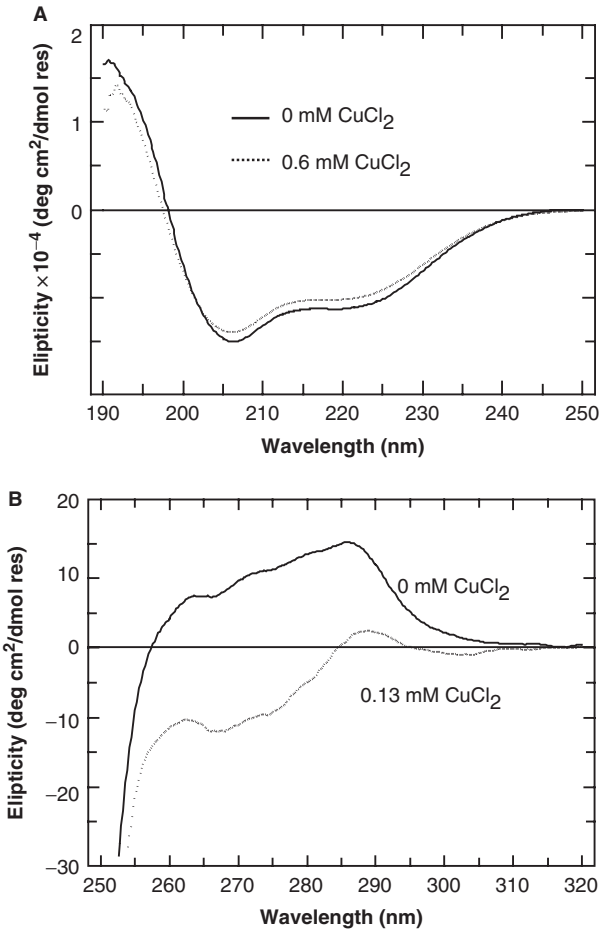

Fig. 5. **CD spectrum analysis of the secondary and tertiary structures of PCaP1.** (A) Far-UV CD spectra for the analysis of secondary structure. Far-UV (190–250 nm) spectra of PCaP1 were monitored in the presence (dashed line) or absence (solid line) of 0.6 mM $CuCl_2$. The PCaP1 concentration was 7.3 μM in 10 mM Tris–HCl (pH 7.5). (B) Near-UV CD spectra in the presence (dashed line) or absence (solid line) of 0.13 mM $CuCl_2$ for the analysis of the tertiary structural change. The PCaP1 concentration was 40.7 μM in 10 mM Tris–HCl (pH 7.5).

elucidate the heat denaturation of PCaP1 (Fig. 6A). The CD spectrum of PCaP1 after cooling to 20°C was restored to the initial spectrum (data not shown). The spectra lacked the typical signature of the β-structure and showed negative peaks at 205 and 222 nm, which are typical for α-helix. A negative signal at 198 nm that is typically found in unstructured proteins (*28–30*) was found at >55°C. With the increase in temperature from 20°C to 70°C, the ellipticity at 205 and 222 nm was gradually decreased and the intensity at 198 nm was concomitantly increased. These results indicate that the content of α-helix decreased and that of the unstructured region increased in the absence of metal ion. Furthermore, there was no change in CD ellipticity at 202 nm by 11,210 degree cm^2 $dmol^{-1}$ in a wide range of temperatures, suggesting that there is an isodichroic point at 202 nm. The isodichroic point means a linear combination of the structural transitions between the two conformational states.

Cu^{2+}-binding form of PCaP1 showed different spectra at >35°C. The ellipticity at 205 and 222 nm gradually decreased with the increase in temperature (Fig. 6B). The CD spectrum at 70°C in the presence and absence of 0.6 mM Cu^{2+} was different (Fig. 6C). These differences in CD spectra are a typical α-helical ones between 20°C and 70°C (20°C – 70°C), regardless of the presence or absence of Cu^{2+} (Fig. 6C, inset). These results indicate that the conformational change of PCaP1 by Cu^{2+} binding was different from that of heat denaturation. When the ellipticity at 220 nm that reflects the content of α-helix was plotted against temperature, the transition temperature was calculated to be 34.6 and 48.7°C for the Cu^{2+}-binding and Cu^{2+}-free form, respectively, from the calibration curve (Fig. 6D). Interestingly, the heat transition of the Cu^{2+}-binding form is sharper despite of the lower transition temperature.

Protease Susceptibility of Cu^{2+}-binding Form of PCaP1—Protease susceptibility of PCaP1 was examined in the presence or absence of metal ions. *Staphylococcus aureus* V8 proteinase, a serine proteinase, catalyses the preferential cleavage at the carboxyl sites of aspartic and glutamic acid residues. A high content of glutamic acid residue is one of the characteristics of PCaP1 and the protein has 46 possible cleavage sites. PCaP1 was digested by V8 proteinase after treatment for 60 min. Calcium and magnesium showed no effect on the proteinase activity, but the presence of Cu^{2+} enhanced markedly the proteolytic digestion of PCaP1 (Fig. 7A and B). This was not due to the activation of V8 proteinase by copper, since addition of Cu^{2+} did not stimulate digestion of ovalbumin by V8 proteinase (data not shown). These results suggest that the mode and/or site of Cu^{2+} binding are different from those of Ca^{2+} and Mg^{2+}.

Static Properties of PCaP1 for Cu^{2+} Binding—The PCaP1 protein solution was titrated with Cu^{2+} solution to determine the binding properties of PCaP1 for Cu^{2+}. The fluorescent peak at 344.8 nm gradually decreased with the increase in the Cu^{2+} concentration from 0.63 to 56.5 μM (Fig. 8A). A double-reciprocal plot of $(F_{H2O} - F_{Cu})^{-1}$ versus $[Cu^{2+}]^{-1}$ yielded a straight line (Fig. 8B) and the association constant (K_a) of PCaP1 for Cu^{2+} and the number of Cu^{2+} bound to a single PCaP1 molecule were calculated to be $\sim 1.0 \times 10^5\ M^{-1}$ (dissociation constant K_d, 10 μM) and 6.1 ions per molecule, respectively. The reversibility of Cu^{2+} binding was examined by re-titration of the PCaP1 sample that was treated with EDTA and subjected to dialysis to remove the bound Cu^{2+} from the protein (data not shown). The obtained values of K_a by the dialysis method was $0.6 \times 10^5\ M^{-1}$ (K_d, 16 μM). There was no difference in K_a values between the titration and dilution methods. Furthermore, binding capacity and affinity to Cu^{2+} were not affected by other ions. The K_a for Cu^{2+} ($1.0 \times 10^5\ M^{-1}$) and the Cu^{2+}-binding number (~6) were not changed even in the presence of Ca^{2+} (K_a for Cu^{2+}, $1.1 \times 10^5\ M^{-1}$), Mg^{2+} (K_a for Cu^{2+}, $1.1 \times 10^5\ M^{-1}$) and K^+ (K_a for Cu^{2+}, $1.0 \times 10^5\ M^{-1}$). These results indicate that PCaP1 reversibly binds a large number of Cu^{2+} ions with high specificity to Cu^{2+}.

We also tried to determine the K_a value and the binding number of Cu^{2+} from the absorption spectra. The solution

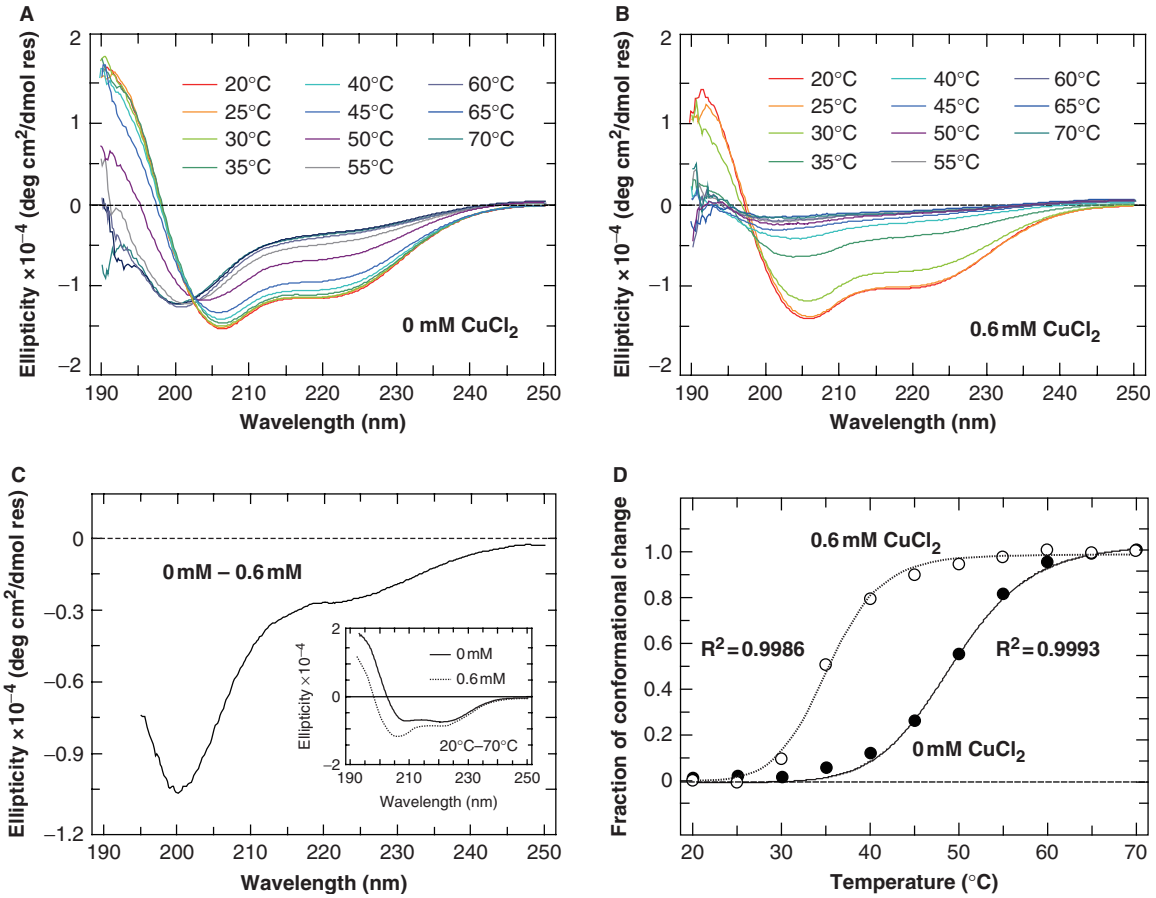

Fig. 6. **Far-UV CD spectrum analysis of PCaP1.** (A) Effect of temperatures on the structure of PCaP1 in the absence of Cu^{2+}. Far-UV CD spectra of PCaP1 (7.3 μM) in 10 mM Tris–HCl (pH 7.5) were obtained at different temperatures from 20°C to 70°C. An apparent isodichroic point was at 202 nm. (B) Far-UV CD spectra of PCaP1 (7.3 μM) in the presence of 0.6 mM $CuCl_2$. (C) Difference CD spectrum of PCaP1 between 0 and 0.6 mM $CuCl_2$ (0 mM − 0.6 mM) at 70°C. *Inset*, different CD spectra of PCaP1 heating from 20°C to 70°C (20°C − 70°C) with (dashed line) or without (solid line) 0.6 mM $CuCl_2$. (D) Conformational change induced by being raised the PCaP1 solution temperature from 20°C to 70°C. The ellipticity of PCaP1 in the presence (open circles) or absence (closed circles) of 0.6 mM $CuCl_2$ at 220 nm was plotted against the temperature. Transition midpoints of PCaP1 in the presence and absence of $CuCl_2$ were 34.9°C and 48.7°C, respectively.

of $CuCl_2$ without protein sample showed typical absorption spectra in a concentration dependent manner (Fig. 9A). Copper ion gave a peak at 634 nm at 50 μM of Cu^{2+} and a peak at 679 nm at 600 μM. When the PCaP1 solution at 58.2 μM was titrated with $CuCl_2$, the peak absorbance was 565 nm at 50 μM Cu^{2+} and 671 nm at 600 μM Cu^{2+} (Fig. 9B). Absorption spectrum of Cu^{2+} depends on the atomic or molecular species of ligand. Ligands for Cu^{2+} are H_2O and Cl^- in water solution without protein, and are changed to H_2O and amino acid residues in the presence of copper-binding protein. The molar ratio of 50 μM Cu^{2+} to 58.2 μM PCaP1 was 0.86. At a high molar ratio of Cu^{2+} to protein, the absorption peak shifted to a longer wavelength as shown in Fig. 9B. A plot of differential wavelength (y) versus the molar ratio of Cu^{2+} to PCaP1 protein (x) fits to the following equation and shows a sigmoid curve (Fig. 9C).

$$y = 0.4291 + \frac{60.647}{1 + \exp[(3.5847 - x)/0.51715]}$$

where, $y = \Delta\lambda = (\lambda_{\text{without-50}} - \lambda_{\text{PCaP1-50}}) - (\lambda_{\text{without}} - \lambda_{\text{PCaP1}})$ (refer the MATERIALS AND METHODS section for the details).

The calculated value of K_a was $1.0 \times 10^5\ M^{-1}$ (K_d, 10 μM) and the binding number was seven Cu^{2+} ions per PCaP1 molecule. This calculation is based on the assumption that Cu^{2+} ions in the solution are bound to PCaP1 at relative low concentrations of Cu^{2+}. The present method has not been established. However, the values are comparable with those (K_d, 10 μM; n, 6) of fluorescence analysis of tryptophan residue in PCaP1 (Fig. 8). Thus, this analysis may support that PCaP1 has ability of binding of relatively large number of Cu^{2+} ions.

DISCUSSION

PCaP1 was found as a novel cation-binding protein and demonstrated to bind Ca^{2+} by ^{45}Ca overlay assay (*6*). During the study, we found that PCaP1 had a capacity to bind copper ion even in the presence of calcium. The aim of this study was to analyse the structural properties of PCaP1 in a Cu^{2+}-binding form and to determine the properties of PCaP1 for Cu^{2+} binding. For the protein

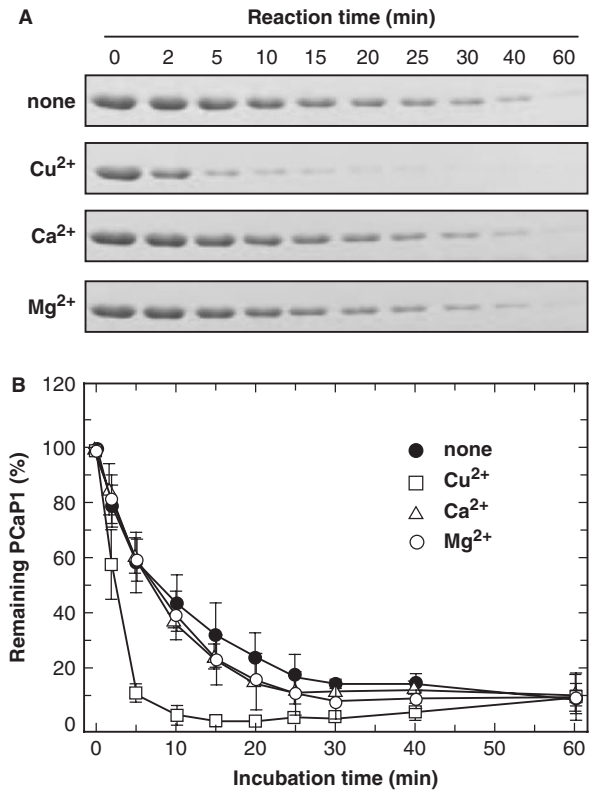

Fig. 7. **Proteinase susceptibility of PCaP1 in the presence of Cu^{2+}.** (A) PCaP1 was treated with V8 proteinase, a *Staphylococcus aureus* proteinase, in the presence of indicated metal ions at 3.3 mM at 37°C for the indicated period and then subjected to SDS–PAGE and staining with Coomassie blue. Metal salts used were $CuCl_2$, $CaCl_2$ and $MgCl_2$ at 3.3 mM. (B) After proteinase treatment and SDS–PAGE, the intensity of stained bands of the intact PCaP1 at 36 kDa was determined densitometrically and plotted against the incubation period. The concentrations of PCaP1 and V8 protease used were 41 μM and 5.7 nM, respectively.

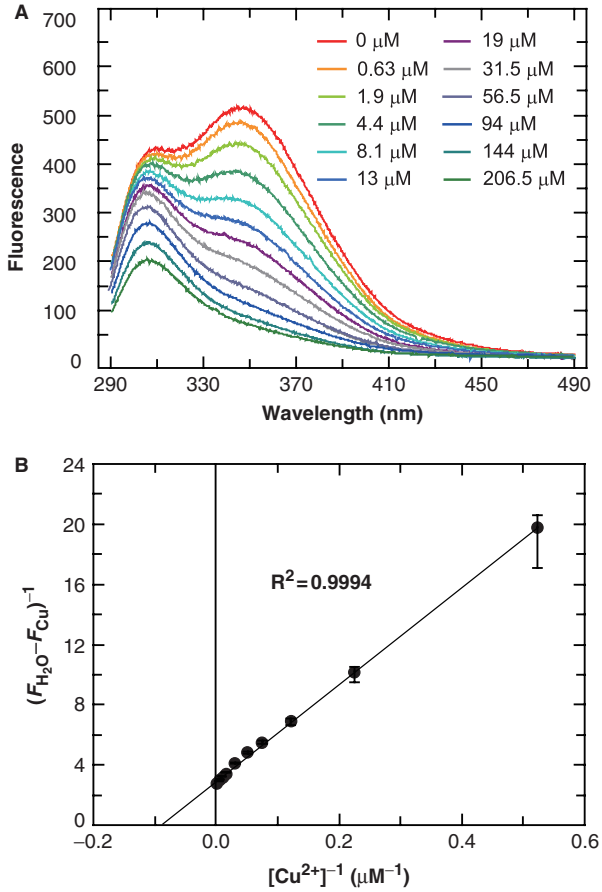

Fig. 8. **Fluorescence spectrum analysis of copper binding to PCaP1.** (A) Fluorescence emission spectra of PCaP1 titrated with $CuCl_2$ at a concentration range of 0–206.5 μM. The concentration of PCaP1 was 0.81 μM in 10 mM Tris–HCl (pH 7.5). (B) Fluorescence at 348.2 nm was determined for both $CuCl_2$ solution (F_{Cu}) and H_2O (F_{H2O}) to quantify the effect of dilution. The value of ($F_{H2O}-F_{Cu}$) was plotted against the concentration of $CuCl_2$ in a double-reciprocal plot. The line was fitted with a double reciprocal equation. The data are the averages of three independent experiments.

physico-chemical analysis, we prepared a large amount of recombinant PCaP1 with no tag peptide or residues.

Basal Structure and Ligand-induced Structural Change of PCaP1—DSC analysis suggests a binding of PCaP1 to Ca^{2+}, Mg^{2+} and Sr^{2+}, because the T_m of the excess heat capacity without the change of denaturation enthalpy as the total excess heat capacity was shifted from 48.6°C to around 46°C when Ca^{2+}, Mg^{2+} or Sr^{2+}, but not K^+, was added (Fig. 1). These results suggest that PCaP1 was more stable at a lower concentration without salt due to entropic destabilization because of only lowering T_m value, which is affected by decreased heat denaturation entropy (*31*). This result indicates that these metal ions induce the structural change of PCaP1 and that the metal ion binding resulted in a slightly unstable form of PCaP1. Several proteins have been reported to become unstable by binding metal ion. The binding of Cu^{2+} to ShaPrP, a prion protein (*32*) and S100A13, a member of the S100 family, (*33*), induced the conformational change to unstable form. The instability caused by the ligand binding is discussed later.

From the physicochemical analyses, PCaP1 has been revealed to have both α-helices and the intrinsically unstructured region as in the basal structure. The negative peaks at 205 and 222 nm indicate the presence of α-helices. A slight negative shoulder and a slight shift to shorter wavelength indicate the presence of the intrinsically unstructured region in PCaP1 (Fig. 6A). The signal for the intrinsically unstructured region at 198 nm appeared clearly in the absence of Cu^{2+}, when the protein was heated at >60°C (Fig. 6A). At high temperatures, α-helices were destroyed and their signal peaks at 205 and 222 nm disappeared. Generally, the intrinsically unstructured state does not show any changes in CD spectrum. Thus, the spectrum was shifted clearly to that of the intrinsically unstructured state at high temperature.

PCaP1 might recover its native structure and ability to bind Ca^{2+} after heat treatment, because the PCaP1 denatured at 70°C reproducibly showed the same DSC pattern as the original pattern without heat denaturation (data not shown) and retained Ca^{2+}-binding capacity (Fig. 2).

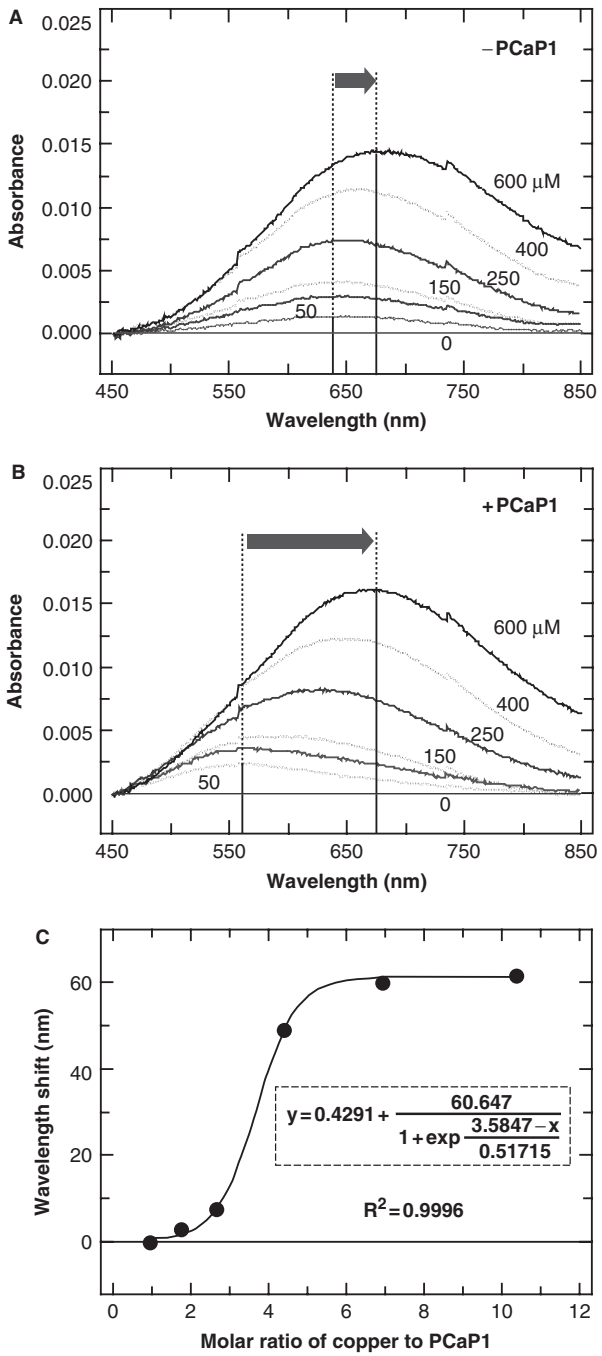

Fig. 9. **Shift of the absorbance wavelength of $CuCl_2$ solution by PCaP1.** (A) Absorption spectra of $CuCl_2$ solution at various concentrations. $CuCl_2$ in 10 mM Tris–HCl (pH 7.5) at final concentrations of 0, 50, 100, 150, 250, 400 and 600 μM was subjected to spectroscopy. (B) Absorption spectra of $CuCl_2$ solution at various concentrations in the presence of PCaP1 (58.2 μM). Arrows indicate the peak wavelength shift at concentration of Cu^{2+} from 50 μM to 600 μM in the absence of PCaP1 (A, 634–679 nm) and the presence of PCaP1 (B, 565–671 nm). (C) Wavelength shift of absorption peak by binding of Cu^{2+} to PCaP1. Values of wavelength shift are plotted as described under the MATERIALS AND METHODS section. Solid line represents the sigmoid curve equation of Cu^{2+}-dependent shift of the absorption peak wavelength. Inset, a theoretical equation representing the relation of the wavelength shift (*y*-axis) to the molar ratio of copper to PCaP1 (*x*-axis).

The capacity of Cu^{2+}-binding has been confirmed for PCaP1 by the following observations: (i) a change in fluorescence absorbance by the presence of Cu^{2+} (Figs 3 and 8), (ii) the temperature-dependent shift of far-UV CD spectrum in the presence of Cu^{2+} (Fig. 6) and (iii) an increase in susceptibility to proteinase by the presence of Cu^{2+} (Fig. 7). The changes in the absorption spectra of Cu^{2+} in the presence of PCaP1 also support the Cu^{2+}-binding ability (Fig. 9). These points are discussed individually.

PCaP1 contains a single residue of tryptophan at position 4 and the peak fluorescence of emission was at 344.8 nm in the absence of metal ions (Fig. 3). This result suggests that this tryptophan is exposed to the hydrophilic surface of the molecule or hydrated. Ca^{2+}, Mg^{2+}, Co^{2+} and Sr^{2+} did not change the intensity of fluorescence at 344.8 nm. However, addition of Cu^{2+} decreased the fluorescence at 344.8 nm, suggesting that the microenvironment surrounding Trp-4 and four tyrosine residues might be changed (Fig. 8) (*26*).

Analysis of the far-UV CD spectrum revealed no change in the secondary structures including α-helix of PCaP1 by binding to Cu^{2+} (Fig. 5). The α-helical structure was clearly detected in the far-UV CD spectrum even in the presence of copper at a low temperature (Fig. 6B). In contrast to this result, near-UV CD analysis revealed that Cu^{2+} binding cause a loss of only typical intrinsically unfolded protein-like structure in the tertiary structure but not the secondary structure of PCaP1 (Fig. 5). A marked change in the near-UV CD spectrum has been reported for a Ca^{2+}-binding protein of radish (*25*). Furthermore, far-UV CD spectra at different temperatures support the association of PCaP1 with Cu^{2+} (Fig. 6). At high temperatures >35°C, the α-helices were broken and a negative peak of the ellipticity was appeared at 198 nm. In the presence of Cu^{2+}, PCaP1 showed a different far-UV CD spectrum. At >50°C, the secondary structural features of PCaP1 were completely lost. In other words, the Cu^{2+}-binding changes the secondary structures including α-helices of PCaP1 at high temperatures.

Characters of Copper Binding—Copper-titration analysis in fluorescence spectroscopy gave the K_d value of 10 μM and the ligand number of approximately six Cu^{2+} ions per PCaP1 molecule (Fig. 8). It should be noted that the Cu^{2+}-binding property was not affected by the existence of other ions such as Ca^{2+}, Mg^{2+} and K^+. In the present study, we applied a new method of wavelength-shift analysis in absorption spectroscopy to determine the Cu^{2+} dissociation constant K_d (Fig. 9). The range of absorption-peak shift reflects the amount of Cu^{2+} bound to the protein in the assay medium. A similar K_d value of 11 μM was obtained by this method. Also, similar value of a ligand-binding number, seven ions per PCaP1 molecule, was obtained by this absorption-peak shift method. Thus, we conclude that PCaP1 has a relatively high capacity of Cu^{2+} binding ($n = 6$ to 7).

The binding sites of copper ions have not been identified in the present study. PCaP1 has 43 glutamate and two aspartate residues, which are localized mainly in the C-terminal half. A large number of these acidic residues might be involved in the high capacity Cu^{2+} binding. Generally, most copper-binding proteins and copper chaperones contain cysteine and/or histidine

residues as a chelator site for copper ion. PCaP1 has neither cysteine nor histidine residue. PCaP1 is the poor propensity to form any secondary structures in the amino acid residues (Tyr, Cys, Phe, Trp, Ile, Leu and Asn) and is rich in the residues that stimulate the formation of the intrinsically unstructured form (Pro, Glu, Lys, Ser and Gln). The content of the latter group residues in PCaP1 is about 50%. Indeed, rod photoreceptors with high glutamate content have been reported to be natively unfolded (*34*). PCaP1 might have a relatively long intrinsically unstructured region. Especially, the C-terminal half (position, 132–225) is rich in polar and charged amino acid residues and lacks bulky hydrophobic residues. This property suggests that the C-terminal half is an intrinsically unstructured region. Indeed, the C-terminal half was predicted to intrinsically unstructured region by the programs of IUPred (*35*) and DISOPRED 2 (*36*). Recently, an unstructured protein of radish RVCaB, which is rich in glutamic acid, has been reported to have high capacity and low-affinity Ca^{2+}-binding properties (*25*). Therefore, we estimate that a large number of glutamate residues in the extended intrinsically unstructured region are involved in the high capacity copper binding.

Partial Similarity of PCaP1 to Prion Protein—Several sequences are known as the copper-binding motifs: namely, Met-*X*-Cys-*X*-*X*-Cys for Cu-ATPase, Cys-*X*-Cys or Cys-*X*-*X*-Cys for copper chaperons, and Pro-His-Gly-Gly-Gly-Trp-Gly-Glu for prion protein (*37*, *38*). These motifs are not detected in PCaP1. Prion protein, a GPI-anchored membrane protein, has a long unstructured region at the N-terminal half and a folded C-terminal half that is rich in α-helices and β-conformation (*39*, *40*). Copper ions bind to the N-terminal half of prion proteins. Although prion protein binds only two ions per molecule, PCaP1 is similar to prion protein in the following biochemical properties (*32*): (i) the structural change was monitored by the far-UV CD analysis in both proteins. Changes in CD spectra of heat denaturation are similar to each other. Spectral analysis revealed that binding of copper causes the structural change to unstable form in both proteins. (ii) The K_d for Cu^{2+} of prion protein (14 μM) is similar to that of PCaP1 (~10 μM). (iii) Prion protein and PCaP1 bind both ions of copper and calcium. (iv) PCaP1 has been estimated to have the intrinsically unstructured region like the N-terminal half of prion protein. Biochemical function of prion protein in normal form (cellular prion, PrP^C) is also unclear like PCaP1. Similarity of the function remains to be examined in the future experiments.

Physiological Meaning of Copper-binding PCaP1—The present study revealed that PCaP1 has a high capacity to bind copper ion with a relatively high affinity. However, we cannot describe the physiological meaning of the copper binding. Previously, PCaP1 has been demonstrated to associate with the plasma membrane through *N*-myristoylation and to interact with phosphatidylinositol phosphates and calmodulin/Ca^{2+} complex (*22*). PCaP1 can transfer Cu^{2+} entered into the cell to copper chaperon(s) at the plasma membrane. Also, PCaP1 can receive the calcium signaling through the interaction with calmodulin/Ca^{2+} complex and/or phosphatidylinositol phosphates and then transmit a signal to other component through physicochemical interaction.

Recently, Patil and Nakamura (*41*) compared 1,662 hub and 4,120 non-hub proteins and proposed that the disordered residues with fewer loops/coils and charged residues confer hubs with the ability to interact with multiple proteins in interaction networks. The hub means a highly connected node for protein–protein interaction networks. PCaP1 is rich in charged residues (glutamate and lysine) and has been demonstrated to contain a relatively large part of the intrinsically unfold regions. The importance of the intrinsically disordered structure has also been discussed in relation to protein function by Dunker *et al*. (*42*). From these comprehensive analyses and the present findings, PCaP1 is proposed as a good candidate for a hub protein at the plasma membrane for signal transduction through Ca^{2+}, Cu^{2+} and phosphatidylinositol phosphates. Studies on the phenotypic properties of the plants over-expressing PCaP1 and the T-DNA-inserted mutant plants are underway for understanding the biochemical function of this novel copper-binding protein.

ACKNOWLEDGEMENT

We are grateful to Mr Yuki Ide for contribution of the initial stage of this study, Dr K. Yutani for characterizing the thermal stability of PCaP1 and Dr Sumiko Kaihara for critical reading of this article.

FUNDING

Grants-in-Aid for Scientific Research from the Ministry of Education, Sports, Culture, Science and Technology of Japan (nos. 16085204, 20380060, and 20657010); GRL program of South Korea; and The Salt Science Research Foundation (no. 0822 to M. Maeshima).

CONFLICT OF INTEREST

None declared.

REFERENCES

1. Nelson, N. (1999) Metal ion transporters and homeostasis. *EMBO J.* **18**, 4361–4371
2. Rodriguez, R.I., Esch, J.J., Hall, A.E., Binder, B.M., Schaller, G.E., and Bleecker, A.B. (1999) A copper cofactor for the ethylene receptor ETR1 from *Arabidopsis*. *Science* **283**, 996–998
3. Horng, Y.-C., Leary, S.C., Cobine, P.A., Young, F.B., Geroge, G.N., Shoubridge, E.A., and Winge, D.R. (2005) Human Sco1 and Sco2 function as copper-binding proteins. *J. Biol. Chem.* **280**, 34113–34122
4. Nishikawa, T., Matsui-Lee, I.S., Shiraishi, N., Ishikawa, T., Ohta, Y., and Nishikimi, M. (1997) Identification of S100b protein as copper-binding protein and its suppression of copper-induced cell damage. *J. Biol. Chem.* **272**, 23037–23041
5. Finney, L.A. and O'Halloran, T.V. (2003) Transition metal speciation in the cell: insights from the chemistry of metal ion receptors. *Science* **300**, 931–936
6. Ide, Y., Nagasaki, N., Tomioka, R., Suito, M., Kamiya, T., and Maeshima, M. (2007) Molecular properties of a novel, hydrophilic cation-binding protein associated with the plasma membrane. *J. Exp. Bot.* **58**, 1173–1183

7. Marschner, H. (1995) *Mineral Nutrition of Higher Plants,* pp. 9.3.1–9.3.6.3, Academic Press, London.
8. Kampfenkel, K., Kushnir, S., Babiychuk, E., Inzé, D., and Van Montagu, M. (1995) Molecular characterization of a putative *Arabidopsis thaliana* copper transporter and its yeast homolog. *J. Biol. Chem.* **270**, 28479–28486
9. Sancenón, V., Puig, S., Mateu-Andrés, I., Dorcey, E., Thiele, D.J., and Peñarrubia, L. (2004) The *Arabidopsis* copper transporter COPT1 functions in root elongation and pollen development. *J. Biol. Chem.* **279**, 15348–15355
10. Seigneurin-Berny, D., Gravot, A., Auroy, P., Mazard, C., Kraut, A., Finazzi, G., Grunwald, D., Rapparport, F., Vavasseur, A., Joyard, J., Richaud, P., and Rolland, N. (2006) HMA1, a new Cu-ATPase of the chloroplast envelope, is essential for growth under adverse light conditions. *J. Biol. Chem.* **281**, 2882–2892
11. Andrés-Colás, N., Sancenón, V., Rodríguez-Navarro, S., Mayo, S., Thiele, D.J., Ecker, J.R., Puig, S., and Peñarrubia, L. (2006) The *Arabidopsis* heavy metal P-type ATPase HMA5 interacts with metallochaperones and functions in copper detoxification of roots. *Plant J.* **45**, 225–236
12. Abdel-Ghany, S.E., Burkhead, J.L., Gogolin, K.A., Andrés-Colás, N., Bodecker, J.R., Puig, S., Peñarrubia, L., and Pilon, M. (2005) AtCCS is a functional homolog of the yeast copper chaperone Ccs1/Lys7. *FEBS Lett.* **579**, 2307–2312
13. Wintz, H. and Vulpe, C. (2002) Plant copper chaperones. *Biochem. Soc. Trans.* **30**, 732–735
14. Burkhead, J.L., Abdel-Ghany, S.E., Morrill, J.M., Pilon-Smits, E.A.H., and Pilon, M. (2003) The *Arabidopsis thaliana CUTA* gene encodes an evolutionarily conserved copper binding chloroplast protein. *Plant J.* **34**, 856–867
15. Balandin, T. and Castresana, C. (2002) AtCOX17, an *Arabidopsis* homolog of the yeast copper chaperone COX17. *Plant Physiol.* **129**, 1852–1857
16. Lin, S. and Culotta, V.C. (1995) The ATX1 gene of *Saccharomyces cerevisiae* encodes a small metal homeostasis factor that protects cells against reactive oxygen toxicity. *Proc. Natl Acad. Sci. USA* **92**, 3784–3788
17. Himelblau, E., Mira, H., Lin, S.J., Culotta, V.C., Peñarrubia, L., and Amasino, R.M. (1998) Identification of a functional homolog of the yeast copper homeostasis gene ATX1 from *Arabidopsis*. *Plant Physiol.* **117**, 1227–1234
18. Culotta, V.C., Klomp, L.W.J., Strain, J., Casareno, R.L.B., Krems, B., and Gitlin, J.D. (1997) The copper chaperone for superoxide dismutase. *J. Biol. Chem.* **272**, 23469–23472
19. Chu, C.C., Lee, W.C., Guo, W.Y., Pan, S.M., Chen, L.J., Li, H.M., and Jinn, T.L. (2005) A copper chaperone for superoxide dismutase that confers three types of copper/zinc super oxide dismutase activity in Arabidopsis. *Plant Physiol.* **139**, 425–436
20. Glenrum, D.M., Shtanko, A., and Tzagoloff, A. (1996) Characterization of *COX17*, a yeast gene involved in copper metabolism and assembly of cytochrome oxidase. *J. Biol. Chem.* **271**, 14504–14509
21. Hall, J.L. (2002) Cellular mechanisms for heavy metal detoxification and tolerance. *J. Exp. Botany* **53**, 1–11
22. Nagasaki, N., Tomioka, R., and Maeshima, M. (2008) A hydrophilic cation-binding protein of *Arabidopsis thaliana* AtPCaP1 is localized to plasma membrane via *N*-myristoylation and interacts with calmodulin and phosphatidylinositol phosphates, PI(3,4,5)P_3 and PI(3,5)P_2. *FEBS J.* **275**, 2267–2282
23. Maruyama, K., Mikawa, T., and Ebashi, S. (1984) Detection of calcium binding proteins by ^{45}Ca autoradiography on nitrocellulose membrane after sodium dodecyl sulfate gel electrophoresis. *J. Biochem.* **95**, 511–519
24. Yuasa, K. and Maeshima, M. (2000) Purification, properties, and molecular cloning of a novel Ca^{2+}-binding protein in radish vacuole. *Plant Physiol.* **124**, 1069–1078
25. Ishijima, J., Nagasaki, N., Maeshima, M., and Miyano, M. (2007) RVCaB, a calcium-binding protein in radish vacuoles, is predominantly an unstructured protein with a polyproline type II helix. *J. Biochem.* **142**, 201–211
26. Pain, R.H. (1998) Determining the fluorescence spectrum of a protein. in *Current Protocols in Protein Science.* (Coligan, J.E., Dunn, B.M., Speicher, D.W., and Wingfield, P.T., eds.), pp. 7.7.1–7.7.20, John Wiley & Sons, Inc., New York.
27. Ohnishi, M., Yamashita, T., and Hiromi, K. (1977) Static and kinetic studies by fluorometry on the interaction between gluconolactone and glucoamylase from *Rh. niveus*. *J. Biochem.* **81**, 99–105
28. Woody, R.W. (1992) Circular dichroism and conformation of unordered peptides. *Adv. Biophys. Chem.* **2**, 37–79
29. Shi, Z., Woody, R.W., and Kallenbach, N.R. (2002) Is polyproline II a major backbone conformation in unfolded proteins? *Adv. Protein Chem.* **62**, 163–240
30. Shi, Z., Olson, C.A., Rose, G.D., Baldwin, R.L., and Kallenbach, N.R. (2002) Polyproline II structure in a sequence of seven alanine residues. *Proc. Natl Acad. Sci. USA* **99**, 9190–9195
31. Plum, G.A. and Breslauer, K.J. (1995) Calorimetry of proteins and nucleic acids. *Curr. Opin. Struc. Biol.* **5**, 682–690
32. Stöckel, J., Safar, J., Wallace, A.C., Cohen, F.E., and Prusiner, S.B. (1998) Prion protein selectively binds copper(II) ions. *Biochemistry.* **37**, 7185–7193
33. Sivaraja, V., Kumar, T.K.S., Rajalingam, D., Graziani, I., Prudovsky, I., and Yu, C. (2006) Copper binding affinity of S100A13, a key component of the FGF-1 nonclassical copper-dependent release complex. *Biophys. J.* **91**, 1832–1843
34. Batra-Safferling, R., Abarca-Heidemann, K., Körschen, H.G., Tziatzios, C., Stoldt, M., Budyak, I., Willbold, D., Schwalbe, H., Klein-Seetharaman, J., and Kaupp, U.B. (2006) Glutamic acid-rich proteins of rod photoreceptors are natively unfolded. *J. Biol. Chem.* **281**, 1449–1460
35. Dosztányi, Z., Csizmók, V., Tompa, P., and Simon, I. (2005) The pairwise energy content estimated from amino acid composition discriminates between folded and intrinsically unstructured proteins. *J. Mol. Biol.* **347**, 827–839
36. Prilusky, J., Felder, C.E., Zeev-Ben-Mordehai, T., Rydberg, E.H., Man, O., Beckmann, J.S., Silman, I., and Sussman, J.L. (2005) Foldindex©: a simple tool to predict whether a given protein sequence is intrinsically unfolded. *Bioinformatics* **21**, 3435–3438
37. Huffman, D.L. and O'Halloran, T.V. (2001) Function, structure, and mechanism of intracellular copper trafficking proteins. *Annu. Rev. Biochem.* **70**, 677–701
38. Hornshaw, M.P., McDermott, J.R., and Candy, J.M. (1995) Copper binding to the N-terminal tandem repeat regions of mammalian and avian prion protein. *Biochem. Biophys. Res. Commun.* **207**, 621–629
39. Riek, R., Hornemann, S., Wider, G., Billeter, M., Glockshuber, R., and Wüthrich, K. (1996) NMR structure of the mouse prion protein domain Prep(121-321). *Nature* **382**, 180–182
40. Donne, D.G., Viles, J.H., Groth, D., Mehlhorn, I., James, T.L., Cohen, F.E., Prusiner, S.B., Wright, P.E., and Dyson, H.J. (1997) Structure of the recombinant full-length hamster prion protein PrP(29-231): the N terminus is highly flexible. *Proc. Natl Acad. Sci. USA* **94**, 13452–13457
41. Patil, A. and Nakamura, H. (2006) Disordered domains and high surface charge confer hubs with the ability to interact with multiple proteins in interaction networks. *FEBS Lett.* **580**, 2041–2045
42. Dunker, A.K., Cortese, M.S., Romero, P., Iakoucheva, L.M., and Uversky, V.N. (2005) Flexible nets: the roles of intrinsic disorder in protein interaction networks. *FEBS J.* **272**, 5129–5148